Plant Soil
DOI 10.1007/s11104-016-2840-2

REGULAR ARTICLE

Allocation of photosynthestically-fixed carbon in plant and soil during growth of reed (*Phragmites australis*) in two saline soils

Ling Li · Shaojun Qiu · Yinping Chen · Xingliang Xu · Ximei Zhao · Peter Christie · Minggang Xu

Received: 19 May 2015 / Accepted: 18 February 2016

Abstract

Aims Terrestrial carbon (C) sequestration is derived mainly from plant photosysthetically-fixed C deposition but soil organic C (SOC) content in saline soils is generally low due to low deposition of C from restricted plant growth. It is important to explore the effects of soil salinity on the allocation of photosynthetically-fixed C to better understand C sequestration in saline wetland soils.

Methods We conducted a pot experiment in which reed (*Phragmites australis*) was grown in a low salinity (LS) soil and a high salinity (HS) soil from the Yellow River Delta under flooded conditions. The allocation of photosynthetically-fixed C into plant tissues, SOC, dissolved organic C (DOC), microbial biomass C (MBC), particulate organic C (POC), and mineral-associated organic C (MAOC) was determined using a ^{13}C pulse-labeling method after four labeling events during the 125-day-long reed growing season and destructive sampling immediately at the end of six hours of pulse labeling (end 6-h) and on the final harvest day (final day).

Results In most cases soil salinity, reed growth stage, or reed biomass significantly ($P < 0.05$) affected the deposition of photosynthetically-fixed C into the plant-soil system. At all four pulses at end 6-h the high salinity soil had significantly ($P < 0.05$) lower percentage net assimilated ^{13}C in the roots and significantly higher ($P < 0.05$) percentage net assimilated ^{13}C in the soil than did the low salinity soil. At both end 6-h and on the final day the high salinity soil had significantly ($P < 0.05$) lower $SO^{13}C$, and significantly ($P < 0.05$) higher $DO^{13}C/SO^{13}C$ ratio than the low salinity soil except for pulses 3 and 4 on the final day. The majority of photosynthetically-fixed C in soil was deposited into MAOC pools and >80 % of deposited $SO^{13}C$ was present as MAOC in the high salinity soil due to its significantly ($P < 0.05$) higher clay content compared with the low salinity soil.

Conclusions Soil salinity affected the allocation of photosynthetically-fixed C in the plant-soil system,

Responsible Editor: Eric Paterson.

Electronic supplementary material The online version of this article (doi:10.1007/s11104-016-2840-2) contains supplementary material, which is available to authorized users.

L. Li · S. Qiu (✉) · M. Xu (✉)
National Engineering Laboratory for Improving Quality of Arable Land, Ministry of Agriculture Key Laboratory of Plant Nutrition and Fertilizers, Institute of Agricultural Resources and Regional Planning, Chinese Academy of Agricultural Sciences, Beijing 100081, China
e-mail: qiushaojun@caas.cn
e-mail: xuminggang@caas.cn

L. Li · Y. Chen · X. Zhao
Shandong Key laboratory of Eco-Enviromental Science for Yellow River Delta, Binzhou University, Binzhou City, Shandong Province 256603, China

X. Xu
Key Laboratory of Ecosystem Network Observation and Modelling, Institute of Geographic Sciences and Natural Resources Research, Chinese Academy of Sciences, Beijing 100101, China

P. Christie
Agri-Food and Biosciences Institute, Belfast BT9 5PX, UK

Published online: 02 March 2016

and soil texture altered the allocation of rhizodeposition C in different soil particles.

Keywords Soil salinity · Soil organic C pools · Photosynthetically-fixed C · ^{13}C pulse labeling · Flooded pot experiment

Introduction

Soil organic carbon (SOC) is the largest terrestrial carbon pool and it represents approximately double the amount of C stored in the atmosphere (Lal 2004). Wetlands contain ~30 % of the terrestrial SOC but they cover >10 % of the terrestrial land surface (Gao et al. 2014) and hence wetlands exert a great influence on the global C cycle. As global warming becomes increasingly important, SOC sequestration by wetlands has been considered to be a potential sink for atmospheric C (Euliss et al., 2006). Saline wetlands characterized by saltwater intrusion affect plant biomass production and deposition (Chambers et al. 2013) and threaten the function of wetlands to serve as C sinks (Chmura et al. 2003; Kirwan and Mudd 2012; Lu et al. 2014). It is therefore important to understand SOC sequestration in saline wetlands.

The majority of SOC in natural terrestrial ecosystems is derived from plants (Kuzyakov et al. 1999; Richert et al. 2000). Numerous studies have shown that about 20–50 % of net photosynthetically-fixed C is allocated to roots (Lynch and Whipps 1990; Kuzyakov and Domanski 2000) and up to 40–90 % of this fraction is retained in the soil (Lu and Conrad 2005). The best methods for investigation of C allocation from plants to soil are C isotopic (^{13}C, ^{14}C) techniques. ^{13}C pulse labeling provides an easily applied method to trace the distribution of recently photosynthetically-fixed C at different stages of plant growth (Kuzyakov and Domanski 2000; Richert et al. 2000; Lu et al. 2002). In recent decades there have been many studies on the translocation of net plant C into the soil in rice systems (Lu et al. 2002), wheat (Kuzyakov and Domanski 2000), reeds (Richert et al. 2000), and pastures (Lynch and Whipps 1990; Kuzyakov and Domanski 2000) but most of these studies have been conducted in non-saline soils. Generally, studies on the responses of soil processes to salinity have used natural saline soils or artificial saline soils with added salt (Conde et al. 2005; Dendooven et al. 2010; Elgharably and Marschner 2011; Li et al. 2012). Natural saline soils can show how salinity affects soil processes and microorganisms, and natural saline soils can avoid the problems of microbial adaptation and SOC release as soil aggregates degrade when salinity is increased in artificially created saline soils. So far, there has been little information on the allocation of photosynthetically-fixed C at different plant growth stages into various C pools in natural saline soils using ^{13}C pulse-labeling techniques.

The soil organic C pool can be classified into active and passive pools. The active pools comprise dissolved organic C (DOC), microbial biomass C (MBC) and particulate organic C (POC) (Qiu et al. 2010). Dissolved organic C originates mainly from root exudates, plant residues, humic substrates and living or dead microorganisms (Kalbitz et al. 2000; Toosi et al. 2012). Soil microorganisms are the driving force of SOC turnover, and MBC reflects the size of the microbial biomass and often correlates with microbial functions in soil C turnover (Jenkinson 1988). Both POC and mineral-associated organic C (MAOC) reflect physical protection in different soil particles (Six et al. 2002; Zeller and Dambrine 2011). Particulate organic C represents a substantial fraction of fresh plant residues and of plant residues at various stages of decomposition. In contrast to POC, MAOC is the residual C after POC removal and is regarded as the relatively stable C pool (Salvo et al. 2010, Briedis et al. 2012; Martins et al. 2012). However, Torn et al. (2013) also report that MAOC contains a fast-turnover C component, and thus it is necessary to further investigate MAOC stability. Dissolved organic C as mobile C in soil provides energy for microorganisms and is adsorbed by soil particles (Kalbitz et al. 2000), and dead microorganisms release DOC or form the relative stable pools (Kalbitz et al. 2003). Soil microorganisms can attach to soil particles (Nicolás et al. 2014) and also utilize C sources from soil particles (Six et al. 2002; Martins et al. 2012; Torn et al. 2013; Keiluweit et al. 2015). Overall, DOC, MBC, POC, and MAOC together represent the chemical, biological, and physical forms of SOM. The analysis of the photosynthetically-fixed C allocated into the various organic C pools above in saline wetland soils can help to better understand the effects of salinity on the biological activity and stability of SOC.

The Yellow River Delta is situated adjacent to the Bohai Sea, is the largest estuarine delta in China, and has a relatively large area of saline wetlands (Liu et al. 2014). Common reed (*Phragmites australis*) is the dominant halophyte in drylands and wetlands in this region (Wang et al. 2002) and it displays a wide range of

salinity tolerance from 5 to 65 ‰ (Engloner 2009; Hurry et al. 2013). *Phragmites australis* can be propagated by both seeds and rhizomes but the latter is the dominant method (Mauchamp et al. 2001; Engloner 2009). Reed is a perennial plant with a well-developed root system and it plays an important role in carbon sequestration in salt marshes (González-Alcaraz et al. 2012). The objectives of the present study were therefore to investigate the effects of soil salinity on the allocation of photosynthetically-fixed C into reed plants and SOC during plant growth under flooded conditions, and to quantify the deposition of photosynthetically-fixed C by reed into DOC, MBC, POC, and MAOC during plant growth. We addressed these questions by conducting a pot experiment in which reed was grown in a natural low salinity (LS) soil and a natural high salinity (HS) soil from the Yellow River Delta under flooded conditions and by analyzing photosynthetically-fixed C allocation using a ^{13}C pulse-labeling technique.

Materials and methods

Site and soil description

The Yellow River Delta is located in the northern part of Shandong province, China, on the southern shore of the Bohai Sea. The region is characterized by a temperate, semi-humid continental monsoon climate with an average annual rainfall of 600 mm, evaporation of 2000 mm, and an annual average temperature of 12.5 °C. Extensive primary salinization is a natural characteristic of this region and is derived from the shallow, saline water table and marine sediments (Wang et al. 2010; Han et al. 2013). The typical soil type is Salic Fluvisol (FAO 2002).

A low salinity soil (LS soil) and a high salinity soil (HS soil) with well-established reed populations were collected from the top 20 cm of the soil profile at adjacent sites in the Yellow River Delta in March 2012. The fresh soils were immediately sieved (< 0.5 cm) and coarse plant residues, roots, and stones were removed. Selected soil physicochemical properties are shown in Table 1.

Experimental design

Using the ^{13}C pulse method (Lu et al. 2002; Ge et al. 2012; An et al. 2015), a pot experiment was carried out from April 22 to August 25 2012 using the LS and HS soils. An internal nylon bag was used for the effective enclosure of the reed roots and rhizosphere soil under flooded conditions and to prevent root growth along the inner wall of the pot. The experiment was carried out in a climate-controlled glass greenhouse. Fresh LS (8.4 kg) or HS soil (9.2 kg), equivalent to 7.6 kg oven-dried soil, was transferred to each pot (25 cm height × 23 cm diameter). Briefly, soil equivalent to 1.6 kg oven-dried basis was added to the bottom of each pot, a nylon bag (25 cm height ×10 cm diameter, 30 μm pore size) filled with soil equivalent to 1.9 kg oven-dried soil was placed into the center of the pot, and then the remaining soil was added to the area around the bag. Before the pot experiment, reed rhizomes were germinated for 14 days in water in a controlled temperature and light room. When shoots were approximately 1.5 cm long, three uniformly sized rhizomes were transplanted at a depth of 2 cm in the soil in the nylon bag in each pot.

Pulse labeling with $^{13}CO_2$ was performed as described by Lu et al. (2002) and Schmitt et al. (2013). On each $^{13}CO_2$ pulse-labeling day, twelve pots of each soil type were transferred to a well-lit airtight chamber (area 150 × 120 cm^2, height 200 cm) and were labeled for 6 h from 8:00 to 14:00. $^{13}CO_2$ was generated in the chamber by a reaction between $Ba^{13}CO_3$ (98 at.% ^{13}C, 12.50 g) and HCl (2 M, 240 ml) in two glass beakers, thereby producing a $^{13}CO_2$ concentration equivalent to about 400 μL L^{-1} at the initial time in the labeling chamber, that is, the total amount of ^{13}C in each pot was calculated to be 33.51 mg according to the chamber volume. Two fans at the top of the chamber distributed the reacted $^{13}CO_2$ evenly throughout the labeling period. A reed stem was circled with a small piece of sponge, a black plastic film covered each pot surface, and elastic was strung outside the circled sponge and the covered film as tightly as possible so that only the reed shoots were directly exposed to the $^{13}CO_2$. During the pulse-labeling treatment in the chamber, 30 extra ice bottles were placed in the chamber to protect the reed tissue from high temperatures (28–42 °C) during the 6-h ^{13}C pulse labeling period. The reeds were pulse-labeled four times with $^{13}CO_2$ on a well-lit sunny day on days 35 (May 27), 55 (June 16), 75 (July 6), and 95 (July 26) after transplanting, namely pulses 1, 2, 3 and 4, correspondingly, the temperature range in the label chamber was 30–40, 30–41, 33–42 and 28–39 °C at the four pulses. A photograph of the $^{13}CO_2$ labeling chamber and the pots inside the chamber during the first 6-h pulse at pulse 1 is shown in Fig. S1.

Table 1 Physicochemical properties of the low salinity (LS) soil and high salinity (HS) soil used in this study

	LS	HS
Location	N 37°49′54.4″ E 18° 08′ 07.3″	N 37°49′52.7″ E 18° 08′ 07.4″
Organic C (g kg^{-1})	4.04 ± 0.13* a	3.47 ± 0.18b
Total N (g kg^{-1})	0.27 ±0.02 a	0.21 ± 0.02b
Mineral N (mg kg^{-1})	26.5 ± 0.3a	18.5 ± 0.8b
Olsen-P (mg kg^{-1})	11.5 ± 0.1a	10.8 ± 0.1b
Exchangeable K (mg kg-1)	655 ± 2a	598 ± 3b
pH	8.15 ± 0.03b	8.33 ± 0.05a
Salinity (%,*w*/w)	0.17 ± 0.02b	1.01 ± 0.03a
Electrolytic conductivity) (μm cm^{-1})	208 ± 7b	2087 ± 59a
Soluble Na^+ (g kg^{-1})	1.0 ± 0.1b	23.5 ± 1.2a
Soluble K^+ (mg kg^{-1})	112 ± 6b	243 ± 7a
Soluble Cl^- (mg kg^{-1})	395 ± 16b	5567 ± 23a
Soluble SO_4^{2-} (mg kg^{-1})	240 ± 9b	844 ± 21a
Soil texture§		
Clay (< 2 μm) (%)	11.8 ± 0.6b	20.3 ± 0.8a
Silt (2-20 μm) (%)	35.9 ± 1.1a	28.5 ± 0.7b
Sand (20–2000) (%)	52.3 ± 1.5a	51.2 ± 1.6a
Coarse particle (>2 μm)		
Hydromica (%)	8.0 ± 0.4a	6.4 ± 0.2b
Chlorite (%)	3.6 ± 0.4a	1.6 ± 0.1b
Quartzite (%)	56.1 ± 1.6a	55.2 ± 1.7a
Feldspar (%)	21.4 ± 1.3a	16.8 ± 0.7b
Clay particle (< 2 μm)		
Smectite (%)	1.7 ± 0.1b	2.8 ± 0.2a
Vermiculite (%)	0.8 ± 0.1a	1.0 ± 0.2a
Hydromica (%)	3.5 ± 0.3b	6.8 ± 0.3a
Kaolinite (%)	2.2 ± 0.1b	4.4 ± 0.4a
Chlorite (%)	2.5 ± 0.2b	4.6 ± 0.4a
Quartzite (%)	0.3 ± 0.1a	0.4 ± 0.1a

* Values are mean ±standard error of three replicates. Different letters in the same row indicate significant difference at $P < 0.05$ between soils

§ Soil texture is based on FAO soil texture classes

The experiment for each soil was a randomized complete block design with 45 replicates. At the four pulse labeling events the number of pots of each soil was 30, with 24 pots for single pulse labeling and 6 pots for repeated pulse labeling. For single pulse labeling, six pots of each soil were destructively sampled at each pulse event, the first three pots were analyzed immediately after 6-h of $^{13}CO_2$ labeling, and the other three pots were sampled later on the final day (August 25, day 125 after reed transplanting). For repeated pulse labeling, they were labeled at all the four pulse ^{13}C labeling events to collect high ^{13}C abundance materials for other experiments. There were a total of 15 control pots of each soil with three unlabeled pots destructively sampled immediately after each pulse event, and the remaining three unlabeled pots were sampled on the final day. The soils were irrigated so that there was a 2–3 cm water layer overlying the soil surface throughout the growing season.

Sampling and analysis

The sampling time was immediately after the 6-h $^{13}CO_2$ pulse labeling and the final harvest day. On the sampling

day the shoots were immediately cut off at the stem base. The main roots were first separated by hand and then the secondary roots were separated on a 0.5-mm sieve with deionized water. Shoots and new roots with rhizomes removed were oven-dried at 60 °C, weighed, and then ball-milled to pass through a 0.25-mm screen. The soil around the roots in the nylon bag was collected and mixed thoroughly. A sub-sample of soil was taken to determine MBC and DOC immediately. The remaining soil was air-dried to determine SOC, POC, and MAOC.

Microbial biomass C was determined by the anaerobic $CHCl_3$ fumigation-extraction method (Inubushi et al. 1991). Fresh soil around the roots was removed in the supernatant water as soon as possible and 0.5 ml $CHCl_3$ was added to the wet soil (50 g on oven-dried basis) to avoid excessive soil water content under the anaerobic conditions impairing the effect of $CHCl_3$ fumigation on soil microorganisms. The mixture was stirred thoroughly and kept in a sealed vacuum desiccator for 24 h. The fumigated soil was evacuated repeatedly in a clean empty desiccator until no further odor of $CHCl_3$ was detected. A 25-g subsample of soil (oven-dried basis) was then extracted with 100 ml 0.5 M K_2SO_4 for 30 min. After extraction, the fumigated filtrate was further boiled for 30 min at 100 °C in a water bath to completely remove any residual $CHCl_3$, and the evaporation loss in the bath was compensated for with deionized water according to weight balance. At the time of sampling of fumigated soil from the pots, non-fumigated soil (the control) was also sampled and extracted with 0.5 M K_2SO_4 in the same way as the fumigated soil. Due to uneven distribution of the ^{13}C label in the microbial biomass during the initial 6 h, MBC was estimated from the difference between the total organic C in the fumigated and non-fumigated extracts without K_{ec} correction. The organic C in the non-fumigated extracted solution was regarded as DOC (Lou et al. 2004; An et al. 2015).

To determine SOC, soil passed through a 0.15-mm mesh sieve was washed with 0.4 M HCl to remove carbonates and 0.4 M HCl was used to avoid the effect of acid on the carbon isotope (Micwood and Boutton 1998). The acid-washed slurry was washed with deionized water until the solution pH reached approximately 6. The mixture was then oven-dried at 60 °C. Both the 0.4 M HCl washing solution and the deionized water were collected, neutralized to pH about 6 with 1 M NaOH solution, transferred to a 500 ml volumetric flask, and filtered to remove any deposits. Organic C in the filtrate was acid soluble organic C (ASOC), and organic C in the acid-washed slurry was acid insoluble organic C (AIOC). The sum of ASOC and AIOC was SOC. The ASOC fraction is not shown in this report because it was a byproduct of SOC determination during acid washing.

Particulate organic C and MAOC were separated as described by Martins et al. (2012). Briefly, 50 g of air-dried soil (< 2 mm) was dispersed for 16 h on a reciprocal shaker in 200 ml deionized water containing 10 glass beads (6-mm diameter). The soil suspension was passed through a 53-μm mesh sieve and rinsed thoroughly with deionized water. The fractions of particles >53 μm and <53 μm were oven-dried at 60 °C. Correspondingly, the organic C in both fractions was defined as POC and MAOC. MAOC was calculated by subtracting POC from SOC to avoid the effect of carbonate in the <53 μm fraction.

Organic C in the 0.5 M K_2SO_4-extracted fumigated and non-fumigated solutions and ASOC were determined using a TOC analyzer (LiquiTOC II, Elementar, Hanau, Germany). Total C and nitrogen (N) in shoots and roots, AIOC, POC, and soil total N were determined with a CN analyzer (VarioEL III, Elementar, Hanau, Germany) after passing samples through a sieve with a 0.25-mm or 0.15-mm mesh. The abundance of ^{13}C in all samples described above was determined with a mass spectrometer (Delta Plus XP, Thermo Finnigan, Bremen, Germany). The solutions containing the samples described above were concentrated into solid form before ^{13}C analysis. Briefly, 0.5 M K_2SO_4-extracted fumigated and non-fumigated solutions were oven-dried at 60 °C and then the residues were ground to pass through a 0.15-mm mesh sieve (Lu et al. 2003; Schmitt et al. 2013; An et al. 2015). For the acid washing solutions, 400 ml was concentrated to 2–3 ml in an oven at 60 °C. The condensed solution was adsorbed onto trapping GD/F glass fiber filter papers (6–8 mm diameter) and then oven-dried at 60 °C.

Before the pot experiment, sieved 2 mm fresh soil from the Yellow River Delta was analyzed for mineral N (NH_4^+-N and NO_3^--N), and sieved 2 mm air-dried soil was analyzed for soluble Na^+, K^+, Cl^-, SO_4^{2-}, pH, electrical conductivity (EC), soil texture, and soil mineralogy. Mineral N was extracted from fresh soil with 0.01 M $CaCl_2$ at a soil:water ratio of 1:10 (*w*/*v*) and determined using an autoanalyzer (AA3, Bran and Luebbe, Norderstedt, Germany). Soluble Na^+ and K^+ contents were determined using an atomic absorption spectrophotometer

(AA-6800, Shimadzu, Kyoto, Japan). Soluble Cl^- and SO_4^{2-} contents were determined using ion chromatography (ICS-2000, Dionex, Sunnyvale, CA). Soil pH was determined in water (1:2.5). Electrical conductivity (EC) was determined in water (1:5). The total salt content in soil was determined by the distillation residue method (Wang et al. 2010). Briefly, soil was extracted for 3 min with deionized water at a ratio of 1:5 (*w*/*v*) on a shaker, then the filtered solution into a porcelain dish was dried in a water bath at 80 °C. H_2O_2 was frequently added to the porcelain dish to remove organic matter during the condensation of the filtered solution. The condensed residue was oven-dried at 105 °C and regarded as the total salt content. The soil composition of K-bearing minerals was determined using an X'Pert-Pro X-ray diffractometer (Rigaku Ultima IV, Tokyo, Japan) with Cu Ka radiation (40 kV, 40 mA) and a graphite filter, from 3.0°to 60.0°at a scan speed of 2.0 min^{-1}. Percentages of clay, silt and sand were determined by a laser particle size analyzer (LS13320, Beckman Coulter, Brea, CA) as described by Wang et al. (2015).

^{13}C calculations

The ^{13}C contents in shoots, roots, AIOC, non-fumigated solution, fumigated solution, and POC were calculated as the difference between ^{13}C in the labeled sample and that in the non-labeled sample, as described by Lu et al. (2002):

$$^{13}C_{sample} = \left[\left(atom\%^{13}C\right)_{labeled} - \left(atom\%^{13}C\right)_{unlabeled}\right] \times C_{sample} \div 100 \quad (1)$$

Where C_{sample} is the total organic C content in shoots, roots, AIOC, ASOC, POC, non-fumigated solution or fumigated solution.

At end 6-h in each pot, the sum of the amounts of ^{13}C in shoots, roots and soils is regarded as net assimilated ^{13}C (Lu et al. 2002):

$$\text{Net assimilated}^{13}C = \left(^{13}C_{shoot} + ^{13}C_{root} + ^{13}C_{soil}\right)_{end\ 6\text{–}h} \quad (2)$$

The percentage distribution of ^{13}C in each pot either at end 6-h or on the final day was calculated as:

$$^{13}C \text{ distribution } (\%) = {}^{13}C_{sample} \div \text{net assimilated}^{13}C \quad (3)$$

In the current study the ^{13}C distribution was calculated only in shoots, roots and SOC.

The ^{13}C recovery in each pot was the sum of the amounts of ^{13}C in the shoots, roots and soil at end 6-h or on the final day accounting for the added ^{13}C in the pulse chamber:

$$^{13}C \text{ recovery} = \left(^{13}C_{shoot} + ^{13}C_{root} + ^{13}C_{soil}\right)_{end\ 6\text{–}h \text{ or final day}} \div \text{added}^{13}C \quad (4)$$

^{13}C in different soil pools was calculated as follows:

$$SO^{13}C = AIO^{13}C + ASO^{13}C \quad (5)$$

$$DO^{13}C = {}^{13}C_{non\text{-}fumigated} \quad (6)$$

$$MAO^{13}C = SO^{13}C - PO^{13}C \quad (7)$$

$$MB^{13}C = \left(^{13}C_{fumigated} - {}^{13}C_{non\text{-}fumigated}\right) \quad (8)$$

Statistical analysis

All data were calculated on an oven-dried weight basis and are shown as the mean of three replicates ± SE. Statistical analysis of all variables was carried out using the SPSS 11.5 software package and significant differences are reported at $P < 0.05$ level. Student's t-test was used to analyze differences in mean values of all variables between LS and HS soils at end 6-h and on the final day.

Results

Shoot and root biomass

During the reed growth period (Fig. 1) the biomass of shoots and roots was significantly ($P < 0.05$) greater in LS than in HS soil. On the final day the shoot and root biomass values were 12.1 and 10.1 g pot^{-1}, respectively, in LS soil, 2.4 and 4.8 times higher than in HS soil. Conversely, the shoot-to-root ratios in HS soil were significantly ($P < 0.05$) higher than in LS soil and they ranged from 1.2 to 2.5 in HS soil and from 0.9 to 1.2 in LS soil.

^{13}C recovery in the plant-soil system

Both at end 6-h and on the final day (Table 2), the ^{13}C recovery in LS soil was significantly higher ($P < 0.05$)

than in HS soil at each pulse. At end 6-h, the ^{13}C recovery in LS soil was 1.3–5.7 times higher than that in HS soil. On the final day, the ^{13}C recovery in LS soil was 2.1–3.9 times higher than that in HS soil. The ^{13}C recovery at end 6-h was significantly ($P < 0.05$) higher than that on the final day in both soils. During the experiment the ^{13}C recovery decreased with reed growth, and significantly ($P < 0.05$) higher recovery was found at pulses 1 and 2 than at pulses 3 and 4 in both soils both at end 6-h and on the final day.

^{13}C allocation in reed shoots, roots and soil

At end 6-h the percentage of net assimilated ^{13}C in the shoots (Fig. 2a) was 83.6–88.2 % in LS soil and 90.9–96.0 % in HS soil at the four pulses, and it in LS soil was significantly lower ($P < 0.05$) than in HS soil at pulses 3 and 4. On the final day the percentage of net assimilated ^{13}C in LS soil was significantly ($P < 0.05$) lower than in HS soil at pulses 2 and 3. At each pulse the percentage of net assimilated ^{13}C in the shoots on the final day represented 35.6–85.8 % of that at end 6-h in LS soil, and the corresponding values in HS soil were 26.5–81.8 %.

At end 6-h the percentage of net assimilated ^{13}C in the roots (Fig. 2b) in LS soil was significantly ($P < 0.05$) higher than in HS soil at each pulse, and it in LS soil was 1.7–13.9 times higher than in HS soil. On the final day the percentage of net assimilated ^{13}C in the roots in LS soil was significantly ($P < 0.05$) higher than in HS soil at pulses 1 and 2. At each pulse the percentage of net assimilated ^{13}C in the roots on the final day increased by 0.2–1.0 times in LS soil and 0.03–18.0 times in HS soil compared to end 6-h.

At end 6-h the percentage of net assimilated ^{13}C in SOC (Fig. 2c) in the LS soil (range 0.9–1.7 %) was significantly ($P < 0.05$) lower than that in HS soil (range 1.8–4.2 %) at each pulse. On the final day the percentage of net assimilated ^{13}C in SOC in LS soil was significantly ($P < 0.05$) lower than that in HS soil at pulses 2 and 4. At each pulse the percentage of net assimilated ^{13}C in SOC on the final day increased by 0.8–2.3 times in LS soil and 0.1–1.3 times in HS soil compared to end 6-h.

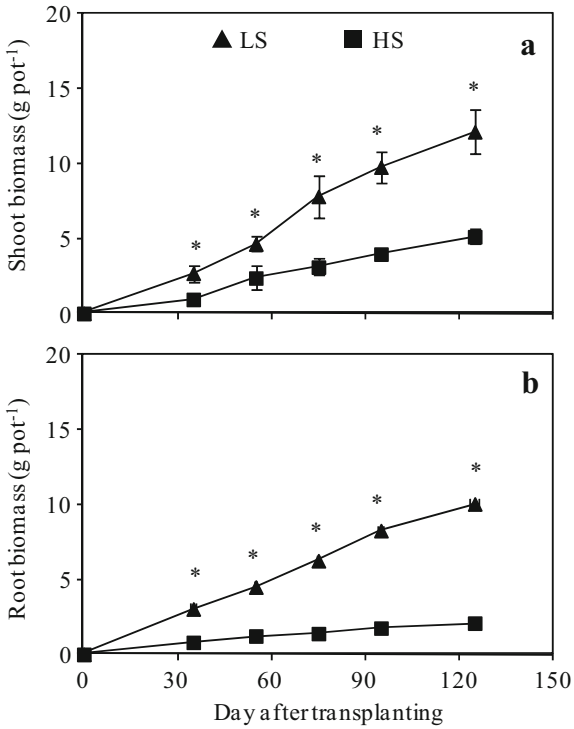

Fig. 1 Biomass of **a** shoots and **b** roots in low salinity (*LS*) and high salinity (*HS*) soils on different days after reed transplanting. *, significant difference ($P < 0.05$) between soils. Bar indicates the standard error of three replicates

$SO^{13}C$ content

Both at end 6-h and on the final day (Fig. 3) the $SO^{13}C$ content in LS soil at each pulse was significantly ($P < 0.05$) higher than that in HS soil. At end 6-h the $SO^{13}C$ content in LS soil was 28.6–119.5 μg kg^{-1} soil during the four pulses and was 1.2–4.2 times higher than that in HS soil. Correspondingly, on the final day (Fig. 3) the $SO^{13}C$ content was 61.1–249.0 μg kg^{-1} soil in LS soil and was 1.3–4.1 times larger than that in HS soil. At each pulse the $SO^{13}C$ content on the final day increased by 0.8–2.1 times in LS soil and 0.3–4.0 times in HS soil compared to end 6-h.

Distribution of $DO^{13}C$ in the $SO^{13}C$ pool

At end 6-h the $DO^{13}C$ as a percentage of $SO^{13}C$ ($DO^{13}C/SO^{13}C$) (Fig. 4) in LS soil (range 1.8–4.4 %) was significantly ($P < 0.05$) lower than that in HS soil (range 3.2–11.4 %) at each pulse. Correspondingly, on the final day in LS soil it was significantly ($P < 0.05$) lower than that in HS soil at pulses 1 and 2. Compared to end 6-h, the $DO^{13}C/SO^{13}C$ on the final day decreased by 47.8–61.2 % from pulses 1 to 3 in LS soil and the corresponding values were 33.8–77.6 % in HS soil. The $DO^{13}C/SO^{13}C$ in both soils at pulse 4 changed little between end 6-h and the final day.

Table 2 ^{13}C recovery in the reed-soil system in two saline soils at the end of 6-h ^{13}C labeling (end 6-h) and on the final harvest day (final day)

Soil	Pulse 1		Pulse 2		Pulse 3		Pulse 4	
	End 6-h	Final day	End 6-h	Final day	End 6-h	Final day	End 6-h	Final day
LS	42.9 ± 4.41 *a	40.9 ± 1.54 a	37.6 ± 2.00 a	23.2 ± 2.20 a	11.1 ± 0.33 a	8.79 ± 0.75 a	19.0 ± 1.02 a	10.4 ± 1.36 a
HS	18.3 ± 0.89 b	13.0 ± 1.86 b	5.59 ± 0.39 b	5.40 ± 0.50 b	1.77 ± 0.07 b	1.99 ± 0.24 b	4.29 ± 0.27 b	2.10 ± 0.30 b

* Values are mean ± standard error of three replicates. Different letters in the same column indicate significant difference at $P < 0.05$ between soils

^{13}C recovery in each pot was calculated as: ^{13}C recovery (%) = ($^{13}C_{shoot} + {}^{13}C_{root} + {}^{13}C_{soil}$) $_{end\ 6\text{-}h\ or\ final\ day}$ ÷ added $^{13}C \times 100$

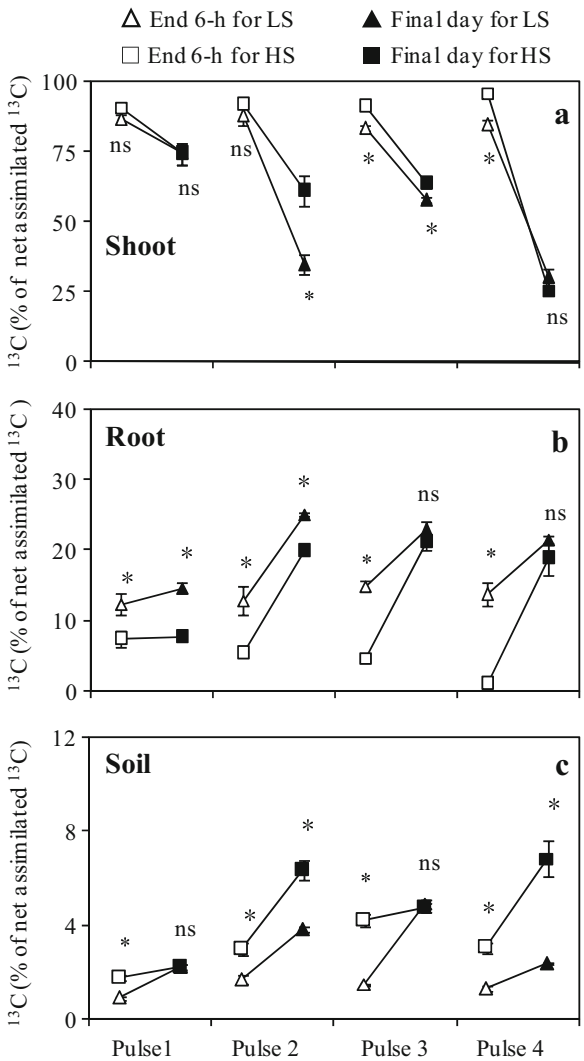

Fig. 2 ^{13}C incorporation in **a** shoots, **b** roots and **c** soil in low salinity soil (*LS*) and high salinity soil (*HS*) at the end of 6-h ^{13}C labeling (end 6-h) and on the final harvest day (final day). *, significant difference ($P < 0.05$) between soils; ns, no-significant difference ($P > 0.05$) between soils. Bar indicates standard error of three replicates

Distribution of $MB^{13}C$ in the $SO^{13}C$ pool

Both at end 6-h and on the final day the $MB^{13}C$ as a percentage of $SO^{13}C$ ($MB^{13}C/SO^{13}C$) (Fig. 5) decreased from pulses 1 to 4 and no significant differences were found between the two soils except for pulse 4 at end 6-h. At end 6-h $MB^{13}C/SO^{13}C$ was 0.8–5.0 % in LS soil and 1.3–5.7 % in HS soil. Compared to end 6-h the $MB^{13}C/SO^{13}C$ on the final day decreased by 58.6–81.8 % from pulses 1 to 3 in LS soil and the corresponding values were 56.4–82.2 % in HS soil.

Distribution of $PO^{13}C$ and $MAO^{13}C$ in the $SO^{13}C$ pool

At end 6-h $PO^{13}C$ (Fig. 6a) was detected in LS soil but was not found in HS soil because of the negative value of ^{13}C abundance between the labeled samples and control samples in HS soil, and $PO^{13}C$ as a percentage of $SO^{13}C$ ($PO^{13}C/SO^{13}C$) in LS soil ranged from 25.7 to 70.1 % during the four pulses. On the final day $PO^{13}C/SO^{13}C$ in

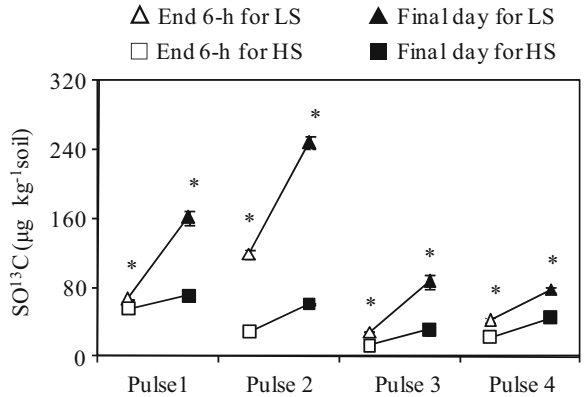

Fig. 3 Content of ^{13}C in soil organic carbon ($SO^{13}C$) in low salinity soil (*LS*) and high salinity soil (*HS*) at the end of 6-h ^{13}C labeling (end 6-h) and on the final harvest day (final day). *, significant difference ($P < 0.05$) between soils. Bar indicates standard error of three replicates

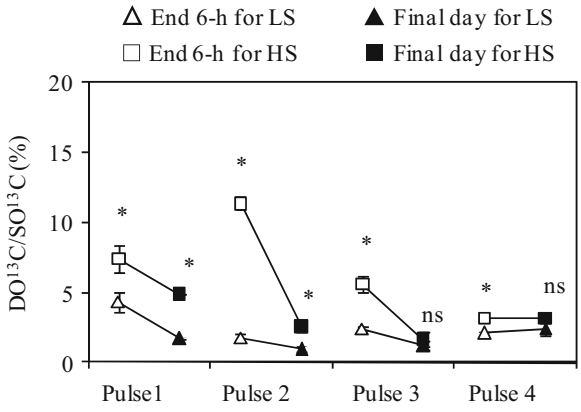

Fig. 4 Percentage of dissolved organic ^{13}C ($DO^{13}C$) in soil organic carbon ($SO^{13}C$) pool in low salinity soil (*LS*) and high salinity soil (*HS*) at the end of 6-h ^{13}C labeling (end 6-h) and on the final harvest day (final day). *, significant difference ($P < 0.05$) between soils; ns, no-significant difference ($P > 0.05$) between soils. Bar indicates standard error of three replicates

LS soil (range 12.7–61.3 %) was significantly ($P < 0.05$) higher than that in HS soil (range 5.6–45.5 %) at each pulse. Compared to end 6-h, $PO^{13}C/SO^{13}C$ in LS soil on the final day increased by 138.3 % at pulse 1 and then decreased by 8.4–81.9 % from pulses 2 to 4.

Both at end 6-h and on the final day (Fig. 6b) the percentage of $MAO^{13}C$ to $SO^{13}C$ ($MAO^{13}C/SO^{13}C$) in LS soil was significantly ($P < 0.05$) lower than that in HS soil at each pulse. At end 6-h the range of $MAO^{13}C/SO^{13}C$ was 29.9–74.3 % in LS soil and 100 % in HS soil. On the final day the range of $MAO^{13}C/SO^{13}C$ was 38.7–87.3 % in LS soil and 54.5–95.4 % in HS soil.

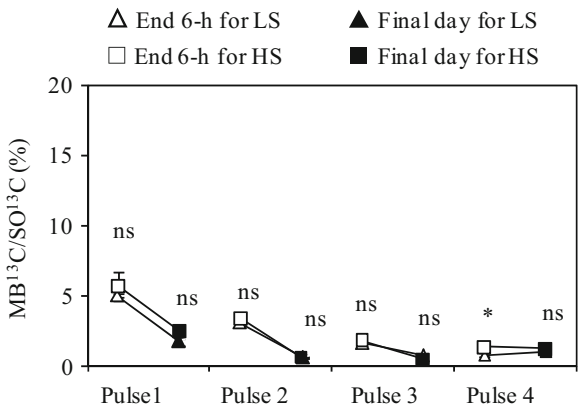

Fig. 5 Percentage of microbial biomass ^{13}C ($MB^{13}C$) in soil organic carbon ($SO^{13}C$) pool in low salinity soil (*LS*) and high salinity soil (*HS*) at the end of 6-h ^{13}C labeling (end 6-h) and on the final harvest day (final day). *, significant difference ($P < 0.05$) between soils; ns, no-significant difference ($P > 0.05$) between soils. Bar indicates standard error of three replicates

Compared to end 6-h, $MAO^{13}C/SO^{13}C$ on the final day decreased in both the soils at pulse 1 and in HS soil at pulse 4 but increased by 91.0–191.9 % ($P < 0.05$) in LS soil at pulses 3 and 4, with no significant change in HS soil at pulses 2 and 3.

Discussion

Effect of soil salinity on reed biomass

Our results show that high soil salinity significantly ($P < 0.05$) inhibited reed biomass production (Fig. 1). This may be due to the relatively high electrical conductivity (EC) and high soluble salt content in HS soil (Table 1) restricting metabolic processes and exudation of hormones from the reeds, possibly further affecting their photosynthesis (Tables 2) (Munns and Tester 2008;

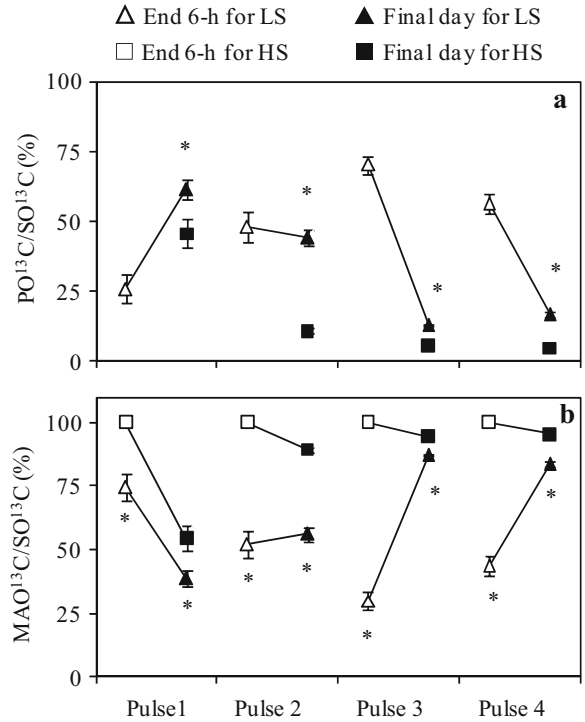

Fig. 6 Percentage of **a** particulate organic ^{13}C ($PO^{13}C$) and **b** mineral associated organic ^{13}C ($MAO^{13}C$) in soil organic carbon ($SO^{13}C$) pool in low salinity soil (*LS*) and high salinity soil (*HS*) at the end of 6-h ^{13}C labeling (end 6-h) and on the final harvest day (final day). *, significant difference ($P < 0.05$) between soils; ns, no-significant difference ($P > 0.05$) between soils. Bar indicates standard error of three replicates. $PO^{13}C$ in HS soil is not shown because of the negative value of ^{13}C abundance between the labeled samples and control samples

Gorai et al. 2010; Yadav et al. 2011). In the present study the concentrations of available nutrients (e.g. mineral N) in HS soil were significantly lower than in LS soil ($P < 0.05$, Table 1), and this may have restricted reed growth (Yadav et al. 2011). Moreover, nutrient uptake by the reeds may have been more restricted in the narrow space in the root bag in our pot experiment than in the natural ecosystem in situ. A similar nutrient-limitation (especially N) effect on growth in pot experiments has also been found in other studies (Lu et al. 2002; Ge et al. 2012; An et al. 2015).

Allocation of photosynthetically-fixed C in the plant-soil system

Net assimilated ^{13}C percentage

High soil salinity can suppress plant growth, restrain photosynthesis, and decrease metabolic processes (Manchanda and Garg 2008; Munns and Tester 2008; Li et al. 2014). For example, Munns and Tester (2008) report that plant response to salinity decreased stomatal aperture and root osmotic activity, stored carbohydrate in leaf cells to mitigate the toxicity of salinity on roots in a saline environment, and further decreased photosynthetically-fixed C flow from aboveground to belowground plant parts with the effect of salinity inhibition of root cell division and expansion, as shown by the higher percentage of net assimilated ^{13}C in shoots in HS soil than in LS soil at all pulses at end 6-h (Fig. 2a). This is also supported by the higher shoot-to-root ratios in HS soil compared with LS soil (Fig. 1), and the lower difference in ^{13}C recovery from end 6-h to the final day at pulses 2 to 4 in HS soil compared with LS soil (Table 2).

In saline soil, roots need to access soil available nutrients and decrease the toxicity due to soil salinity by root secretion during plant growth (Munns and Tester 2008; Morrissey et al. 2014). Moreover, plant senescence on the final day may have released more organic compounds from root cells and tissues into the soil (Pausch et al. 2013; McNally et al. 2015). Thus, the percentage of net assimilated ^{13}C showed a decrease in the shoots as well as increases in the roots and soil (Fig. 2 and S2). However, from end 6-h to the final day the range of net assimilated ^{13}C percentage in the shoots, roots and soil at pulse 1 was lower than at the other three pulses (Fig. 2) and this might be attributable to the reuse or transformation of photosynthetic compounds in the plants because of nutrient limitation due to rapid plant growth (Johnson et al. 2002; Lu et al. 2002; Engloner 2009). This is supported by the higher ^{13}C recovery at pulse 1 than at the other three pulse labeling times (Table 2). An et al. (2015) also report that nutrient-limited treatments had a higher net assimilated ^{13}C percentage in shoots than did fertilization treatments as a result of normal metabolic processes under a sufficient supply of nutrients.

At pulse 2 from end 6-h to the final day the higher root biomass in LS soil than HS soil (Fig. 1) required more photosynthetically-fixed C transfer from aboveground to belowground and this resulted in a significantly ($P < 0.05$) larger range of net assimilated ^{13}C percentage in the shoots between end 6-h and the final day in LS soil compared to HS soil (Fig. 2a).

At pulse 4 from end 6-h to the final day, soil nutrients might be deficient compared to the other three pulses at end 6-h due to greater plant nutrient uptake. As a result, high photosynthetically-fixed C was deposited belowground from the shoots (Figs. 2 and S2) to maintain high microbial activity for mining of soil nutrients and to meet the reed nutrient demand (e.g. N uptake in Fig. S3). This phenomenon resulted in a wide range of net assimilated ^{13}C percentage in shoots between end 6-h and the final day at pulse 4 (Fig. 2a). Warembourg and Estelrich (2001) also reported a greater proportion of C allocation deposited belowground in lower soil fertility conditions. Correspondingly, the percentage of net assimilated ^{13}C in the roots increased (Fig. 2b) on the final day.

In addition, individual differences also affected the percentage of net assimilated ^{13}C from end 6-h to the final day due to the destructive sampling in our study (Fig. 2). For example, the net assimilated ^{13}C percentage for the both soils was not significant in the shoots at end 6-h and on the final day at pulse 1 (Fig. 2a), in the shoots at end 6-h at pulse 2, and in the roots on the final day at pulses 3 and 4 (Fig. 2b), but the general trend of net assimilated ^{13}C percentage in the plant-soil system (Fig. 2) through the influence of soil salinity in both soils would have remained unaffected.

In our study, the reeds encountered high temperatures during the ^{13}C pulse labeling process. High temperatures can inhibit photosynthesis, decrease photosynthesized C fixation and increase photosynthetically-fixed C flow from aboveground to belowground parts (Rennenberg et al. 2006; Bhattacharyya et al. 2013). However, sufficient soil moisture can offset the negative effect caused by high temperatures (Bassirirad et al. 1991; Kuzyakov

and Gavrichkova 2010), such as flooded pot conditions during reed growth. Furthermore, the 6-h pulse labeling was transient comparing the whole 125 d growth stage, and the ^{13}C pulse labeling in both the soils occurred in the same chamber at the same time. Therefore, any effect due to increased temperatures in the chamber can be ignored for the purpose of comparing the allocation of photosynthetically-fixed C in both soils.

$SO^{13}C$

Root exudates and dead root tissues are important sources of SOC during plant growth, especially in natural ecosystems (Kuzyakov and Domanski, 2000; Dijkstra et al. 2006). In most cases in the present study the high salinity in HS soil resulted in a significantly higher net assimilated ^{13}C percentage in soil (Fig. 2c) compared to LS soil. The roots release more exudates to alleviate the toxicity of salinity (Manchanda and Garg 2008; Li et al. 2014) for the normal reed lifecycle in HS soil. For example, there was a significantly higher $DO^{13}C/SO^{13}C$ in HS soil than LS soil (Fig. 4). However, the $SO^{13}C$ content (Fig. 3) depends mainly on plant biomass (McNally et al. 2015). In our study, there was a significant positive correlation between the $SO^{13}C$ content and root biomass (Fig. 7), and there was a significantly ($P < 0.05$) higher $SO^{13}C$ content in LS soil at end 6-h and on the final day compared to HS soil (Fig. 3). The increase in net assimilated ^{13}C percentage in $SO^{13}C$ (Fig. 2c) and $SO^{13}C$ content (Fig. 3) from end 6-h to the final day further indicates that substantial photosynthetically-fixed C enters the SOC pools (Pausch et al. 2013; McNally et al. 2015), but microbial respiration can decrease the actual amount of $SO^{13}C$ deposited (Bahn et al. 2009; Kuzyakov and Gavrichkova 2010).

Allocation of photosynthetically-fixed C in various SOC pools

$DO^{13}C$ and $MB^{13}C$

Both DOC and MBC are important active C pools in soil C biological processes. In comparison with pulses 3 and 4 (Figs.4 and 5), the larger ranges of $DO^{13}C/SO^{13}C$ and $MB^{13}C/SO^{13}C$ from end 6-h to the final day at pulses 1 and 2 was due firstly to younger reed roots having more activity than older roots (Lu et al. 2002; An et al. 2015). Secondly, the ^{13}C contribution was diluted by the newly unlabeled photosynthetically-fixed C as reed growth proceeded (Rangel-Castro et al. 2004). Thirdly, the stronger nutrient competitive abilities for reed demand resulted in smaller size of the rhizosphere microbial biomass (Blagodatskaya et al. 2010; Kuzyakov and Blagodatskaya 2015) during reed growth, as shown by the reed N uptake under the N-limited condition in our study (Fig. S3). Similarly, the inhibition effect of salinity on microorganisms, and more low molecular compounds from roots to activate soil nutrients for reed demand might be the main explanation for the higher percentage of $DO^{13}C/SO^{13}C$ than $MB^{13}C/SO^{13}C$ in both soils in most cases (Blagodatskaya et al. 2010; Mavi et al. 2012).

From end 6-h to the final day, the decreases in $DO^{13}C/SO^{13}C$ (Fig. 4) and $MB^{13}C/SO^{13}C$ (Fig. 5) in both soils might reflect a change from the exudation of easily decomposed root materials to stable recalcitrant forms of C thus contributing to a build-up of soil aggregates (Ge et al. 2012) or losses by soil respiration (Meng et al. 2013). Compared to LS soil, the significantly ($P < 0.05$) higher $DO^{13}C/SO^{13}C$ (Fig. 4) in HS soil may have been due to the roots exuding more organic compounds to resist the negative effects of high salinity on reed growth. In most cases at all pulses the lack of a significant difference in $MB^{13}C/SO^{13}C$ (Fig. 5) in both soils might be attributable to the increased DOC with higher salinity in HS soil masking the adverse effects of soil salinity, providing additional available C sources for microorganisms (Wong et al. 2010), although both at end 6-h and on the final day the size of the total MBC and most of the $MB^{13}C$ in LS soil was larger than that in HS soil (Fig. S4).

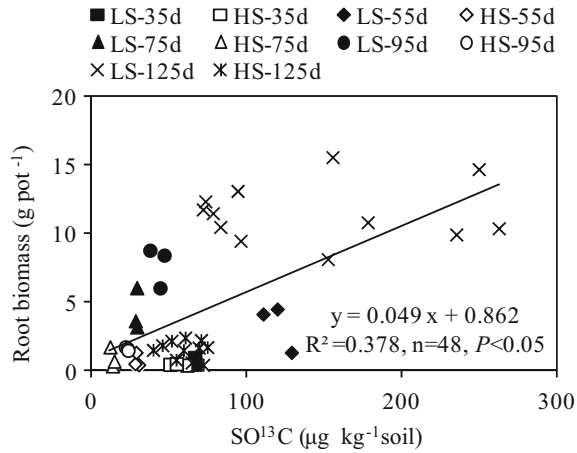

Fig. 7 Relationship between $SO^{13}C$ content and reed root biomass during the reed life cycle

In addition, the rhizosphere transformed to the detritusphere with root death or root development, accordingly, the low-molecular-weight materials from root deposition became recalcitrant highly polymeric compounds, the microbial turnover rate of root-deposited C decreased (Kuzyakov and Blagodatskaya 2015). Consequently, the duration of root-deposited C in the earlier pulses will increase on the final day.

$PO^{13}C$ and $MAO^{13}C$

Particulate organic C is labile organic C and is mainly derived from microbial debris and root residues (Briedis et al. 2012; Martins et al. 2012) but MAOC is relatively resistant organic C and plays a key role in preserving the soil organic C content (Angers et al. 1997; Six et al. 2002; Zeller and Dambrine 2011; Briedis et al. 2012). At end 6-h the disappearance of $PO^{13}C$ in HS soil (Fig. 6a) and more than 70 % of $MAO^{13}C/SO^{13}C$ at pulse 1 in both soils (Fig. 6b) indicate that the majority of deposited $SO^{13}C$ appeared in the <53 μm soil fraction. This is in accord with several previous studies (Angers et al. 1997; Denef et al. 2001) which also report that most plant-derived C was deposited in soil micro-particles rather than macro-particles. At all pulses both at end 6-h and on the final day, the significantly ($P < 0.05$) higher $MAO^{13}C/SO^{13}C$ in HS soil in comparison with LS soil (Fig. 6b) may be related to the differences between the soils in soil texture and clay mineralogy (Barré et al. 2014). Soil clay has higher particle surface area than silt, and soils with higher clay contents can adsorb more C derived from newly formed low molecular compounds (Amato and Ladd 1992; Gonzalez and Laird 2003), as shown by the 1.7 times significantly higher clay content with higher particle surface area in HS soil than in LS soil ($P < 0.05$, Table 1). The minerals of clay fractions can fix the C deposited, such as smectite, hydromica and kaolinite (Six et al. 2002; Saidy et al. 2012), and the contents of smectite, hydromica and kaolinite in HS soil were 64.7, 94.3 and 100 % higher than in LS soil in our study (Table 1).

Particulate organic C is vulnerable to decomposition in the absence of macrostrcuture protection and eventually a partially decomposed POC becomes MAOC (Six et al. 2002; Guan et al. 2015), as shown by the decrease in $PO^{13}C/SO^{13}C$ (Fig. 6a) and the increase in $MAO^{13}C/SO^{13}C$ (Fig. 6b) in LS soil from end 6-h to the final day at pulses 2 to 4. On the other hand, $PO^{13}C/SO^{13}C$ in HS soil increased (Fig. 6a) on the final day and $MAO^{13}C/SO^{13}C$ decreased in LS soil from end 6-h to the final day at pulse 1 (Fig. 6b). This may be attributable to the turnover of microbial biomass induced by the rhizodeposited bio-available DOC (Torn et al. 2013; Keiluweit et al. 2015) or to the sorption and desorption of soil mineral-associated C by physico-chemical processes (Six et al. 2002; Saidy et al. 2012). Some studies also report that the heterogeneous MAOC pool contains fast-cycling C components (Six et al. 2002; Torn et al. 2013; Keiluweit et al. 2015) and the released clay particle C further forms macroaggregate C by microbially-derived organic cementing agents (Six et al. 2002; Denef and Six 2005). Six et al. (2002) also documented that fixed C in 1:1 clay had lower stability than 2:1 clay, as shown by the higher kaolinite content in HS soil than LS soil ($P < 0.05$, Table 1). Hence, both biotic and abiotic mechanisms affect the transformation and allocation of C rhizodeposited in different soil particles.

Conclusions

Soil salinity and pulse events affected the allocation of photosynthetically-fixed C in the plant–soil system during reed growth. High salinity inhibited or altered the photosynthetically-fixed C transported from aboveground (shoots) to belowground (roots and soil) parts of the system. Rhizodeposition is an important donor of C for the formation of SOC in natural saline soils and the young stages of reed (pulses 1 and 2) deposited more C from the plants than did the later stages (pulses 3 and 4). Compared to LS soil, the low root biomass of reed in HS soil resulted in a significantly ($P < 0.05$) lower content of newly formed SOC (Fig. 3), and high soil salinity significantly ($P < 0.05$) increased $DO^{13}C/SO^{13}C$ (Fig. 4) and stimulated the deposition of photosynthetically-fixed C in mineral-associated organic C pools with high clay content and smectite, hydromica and kaolinite content. Soil salinity therefore affected the quantity of deposited C, and soil texture altered the allocation of rhizodeposition C in different soil particles. This study suggests that a better understanding of the effects of salinity on soil C storage is required in relation to C transformation and stabilization in various soil pools closely linked with the contribution of plant growth and soil available nutrients (Six et al. 2002; Xiao et al. 2007; Kuzyakov and Blagodatskaya 2015). Further studies are required on the C storage potential and C stability and availability in MAOC pools.

Acknowledgments This work was funded by the National Natural Science Foundation of China (41101220), the Outstanding Young Scientist Research Award Fund of Shandong Province, China (BS2011HZ001), the "973" program (2013CB127405), and National Nonprofit Institute Research Grant of CAAS (IARRP-2015-27).

References

Amato M, Ladd JN (1992) Decomposition of C-14 labeled glucose and legume material in soil–properties influencing the accumulation of organic residue-C and microbial biomass-C. Soil Biol Biochem 24:455–464

An T, Schaeffer S, Li S, Fu S, Pei J, Li H, Zhuang J, Radosevich M, Wang J (2015) Carbon fluxes from plants to soil and dynamics of microbial immobilization under plastic film mulching and fertilizer application using ^{13}C pulse-labeling. Soil Biol Biochem 80:53–61

Angers DA, Recous S, Aita C (1997) Fate of carbon and nitrogen in water-stable aggregates during decomposition of $^{13}C^{15}N$-labelled wheat straw in situ. Eur J Soil Sci 48:295–300

Bahn M, Schmitt M, Siegwolf R, Richter A, Brüggemann N (2009) Does photosynthesis affect grassland soil-respired CO_2 and its carbon isotope composition on a diurnal timescale? New Phytol 182:451–460

Bassirirad H, Radin JW, Matsuda K (1991) Temperature dependent water and ion-transport properties of barley and Sorghum roots. 1. Relationship to leaf growth. Plant Physiol 97:426–432

Bhattacharyya P, Roy KS, Neogi S, Manna MC, Adhya TK, Rao KS, Nayak AK (2013) Influence of elevated carbon dioxide and temperature on belowground carbon allocation and enzyme activities in tropical flooded soil planted with rice. Environ Monit Assess 185:8659–8671

Barré P, Fernandez-Ugalde O, Virto I, Velde B, Chenu C (2014) Impact of phyllosilicate mineralogy on organic carbon stabilization in soils: incomplete knowledge and exciting prospects. Geoderma 235–236:382–395

Blagodatskaya E, Littschwager J, Lauerer M, Kuzyakov Y (2010) Growth rates of rhizosphere microorganisms depend on competitive abilities of plants and N supply. Plant Biosyst 144:408–413

Briedis C, Sá JCM, Caires EF, Navarro JF, Inagaki TM, Boer A, Neto CQ, Ferreira AO, Canalli LB, Santos JB (2012) Soil organic matter pools and carbon-protection mechanisms in aggregate classes influenced by surface liming in a no-till system. Geoderma 170:80–88

Chambers LG, Osborne TZ, Reddy KR (2013) Effect of salinity-altering pulsing events on soil organic carbon loss along an intertidal wetland gradient: a laboratory experiment. Biogeochemistry 115:363–383

Chmura GL, Anisfeld SC, Cahoon DR, Lynch JC (2003) Global carbon sequestration in tidal, saline wetland soils. Global Biogeochem Cy 17:GB1111. doi:10.1029/2002GB001917

Conde E, Cardenas M, Ponce-Mendoza A, Luna-Guido ML, Cruz-Mondragón C, Dendooven L (2005) The impacts of inorganic nitrogen application on mineralization of ^{14}C-labelled maize and glucose, and on priming effect in saline alkaline soil. Soil Biol Biochem 37:681–691

Dendooven L, Alcántare-Hernández RJ, Valenzuela-Encinas C, Valenzuela-Encinas C, Luna-Guido M, Ferez-Guevara F, Marsh R (2010) Dynamics of carbon and nitrogen in an extreme alkaline saline soil: A review. Soil Biol Biochem 42:865–877

Denef K, Six J (2005) Clay mineralogy determines the importance of biological versus abiotic processes for macroaggregate formation and stabilization. Eur J Soil Sci 56:469–479

Denef K, Six J, Bossuyt H, Frey SD, Elliott ET, Merckx R, Paustian K (2001) Influence of dry-wet cycles on the interrelationship between aggregate, particulate organic matter, and microbial community dynamics. Soil Biol Biochem 33:1599–1611

Dijkstra FA, Cheng W, Johnson DW (2006) Plant biomass influences rhizosphere priming effects on soil organic matter decomposition in two differently managed soils. Soil Biol Biochem 38:2519–2526

Elgharably A, Marschner P (2011) Microbial activity and biomass and N and P availability in a saline sandy loam amended with inorganic N and lupin residues. Eur J Soil Biol 47:310–315

Engloner AI (2009) Structure, growth dynamics and biomass of reed (*Phragmites australis*) – A review. Flora 204:331–346

Euliss NH Jr, Gleason RA, Olness A, McDougal RL, Murkin HR, Robarts RD, Bourbonniere RA, Warner BG (2006) North American prairie wetlands are important nonforested land-based carbon storage sites. Sci Total Environ 361:179–188

FAO (2002) Key to the FAO soil units in the FAO/Unesco soil map of the world. Available at www.fao.org/ag/agl/agll/key2soil.stm (verified 17 Nov. 2011). FAO, Rome

Gao J, Lei G, Zhang X, Wang G (2014) Can $\delta^{13}C$ abundance, water-soluble carbon, and light fraction carbon be potential indicators of soil organic carbon dynamics in Zoigê wetland? Catena 119:21–27

Ge T, Yuan H, Zhu H, Wu X, Nie S, Liu C, Tong C, Wu J, Brookes P (2012) Biological carbon assimilation and dynamics in a flooded rice-soil system. Soil Biol Biochem 48:39–46

Gonzalez JM, Laird DA (2003) Carbon sequestration in clay mineral fractions from C-14-labeled plant residues. Soil Sci Soc Am J 67:1715–1720

González-Alcaraz MN, Egea C, Jiménez-Cárceles FJ, Párraga I, María-Cervantes A, Delgado MJ, Álvarez-Rogel J (2012) Storage of organic carbon, nitrogen and phosphorus in the soil-plant system of *Phragmites australis* stands from a eutrophicated Mediterranean salt marsh. Geoderma 185–186:61–67

Gorai M, Ennajeh M, Khemira H, Neffati M (2010) Combined effect of NaCl-salinity and hypoxia on growth, photosynthesis, water relations and solute accumulation in *Phragmites australis* plants. Flora 205:462–470

Guan S, Dou S, Chen G, Wang G, Zhuang J (2015) Isotopic characterization of sequestration and transformation of plant residue carbon in relation to soil aggregation dynamics. Appl Soil Ecol 96:18–24

Han G, Yang L, Yu J, Wang G, Mao P, Gao Y (2013) Environmental controls on net ecosystem CO_2 exchange over a Reed (*Phragmites australis*) wetland in the Yellow River Delta, China. Estuar Coasts 36:401–413

Hurry CR, James EA, Thompson RM (2013) Connectivity, genetic structure and stress response of *Phragmites australis*: Issues for restoration in a salinising wetland system. Aquat Bot 104:138–146

Inubushi K, Brookes PC, Jenkinson DS (1991) Soil microbial biomass C, N and ninhydrin-N in aerobic and anerobic soil measured by the fumigation-extraction method. Soil Biol Biochem 23:737–741

Jenkinson DS (1988) Determination of microbial biomass carbon and nitrogen in soil. In: Wilson JR (ed) Advances in nitrogen cycling in agricultural ecosystems. CAB International, Wallingford, UK, pp. 368–386

Johnson D, Leake JR, Ostle N, Ineson P, Read DJ (2002) In situ $^{13}CO_2$ pulse-labelling of upland grassland demonstrates a rapid pathway of carbon flux from arbuscular mycorrhizal mycelia to the soil. New Phytol 153:327–334

Kalbitz K, Schmerwitz J, Schwesig D, Matzner E (2003) Biodegradation of soil-derived dissolved organic matter as related to its properties. Geoderma 113:273–291

Kalbitz K, Solinger S, Park JH, Michalzik B, Matzner E (2000) Controls on the dynamics of dissolved organic matter in soils: a review. Soil Sci 165:277–304

Keiluweit M, Bougoure JJ, Nico PS, Pett-Ridge J, Weber PK, Kleber M (2015) Mineral protection of soil carbon counteracted by root exudates. Nat Clim Chang. doi:10.1038/NCLIMATE2580

Kirwan ML, Mudd SM (2012) Responses of salt-marsh carbon accumulation to climate change. Nature 489:550–553

Kuzyakov Y, Blagodatskaya E (2015) Microbial hotspots and hot moments in soil: Concept & review. Soil Biol Biochem 83: 184–199

Kuzyakov Y, Domanski G (2000) Carbon input by plants into the soil. Review J Plant Nutri Soil Sci 163:421–431

Kuzyakov Y, Gavrichkova O (2010) Time lag between photosynthesis and carbon dioxide efflux from soil: a review of mechanisms and controls. Glob Chang Biol 16:3386–3406

Kuzyakov Y, Kretzschmar A, Stahr K (1999) Contribution of *Lolium perenne* rhizodeposition to carbon turnover of pasture soil. Plant Soil 231:127–136

Lal R (2004) Soil carbon sequestration impacts on global climate change and food security. Science 304:1623–1627

Li J, Pu L, Zhu M, Zhang J, Li P, Dai X, Xu Y, Liu L (2014) Evolution of soil properties following reclamation in coastal areas: A review. Geoderma 226-227: 130–139

Li XG, Shi XM, Wang DJ, Zhou W (2012) Effect of alkalized magnesic salinity on soil respiration changes with substrate availability and incubation time. Biol Fertil Soils 48:597–602

Liu G, Zhang L, Zhang Q, Musyimi Z, Jiang Q (2014) Spatiotemporal dynamics of wetland landscape patterns based on remote sensing in Yellow River Delta, China. Wetlands 34:787–801

Lou Y, Li Z, Zhang T, Liang Y (2004) CO_2 emissions from subtropical arable soils of China. Soil Biol Biochem 36: 1835–1842

Lu Q, Gao Z, Zhao Z, Ning J, Bi X (2014) Dynamics of wetlands and their effects on carbon emissions in China coastal region – Case study in Bohai Economic Rim. Ocean Coast Manag 87:61–67

Lu Y, Conrad R (2005) In situ stable isotope probing of methanogenic archaea in the rice rhizosphere. Science 309:1088

Lu Y, Watanabe A, Kimura M (2002) Input and distribution of photosynthesized carbon in a flooded rice soil. Global Biogeochem Cy 16:321–328

Lu Y, Watanabe A, Kimura M (2003) Carbon dynamics of rhizodeposits, root- and shoot-residues in a rice soil. Soil Biol Biochem 35:1223–1230

Lynch JM, Whipps JM (1990) Substrate flow in the rhizosphere. Plant Soil 129:1–10

Manchanda G, Garg N (2008) Salinity and its effects on the functional biology of legumes. Acta Physiol Plant 30: 595–618

Martins MR, Angers DA, Corá JE (2012) Co-accumulation of microbial residues and particulate organic matter in the surface layer of a no-till Oxisol under different crops. Soil Biol Biochem 50:208–213

Mauchamp A, Blanch S, Grillas P (2001) Effects of submergence on the growth of *Phragmites australis* seedlings. Aquat Bot 69:147–164

Mavi MS, Marschner P, Chittleborough DJ, Cox JM, Sanderman J (2012) Salinitiy and sodicity affect soil respiration and dissolved organic matter dynamics differentially in soils varying in texture. Soil Biol Biochem 45:8–13

McNally SR, Laughlin DC, Rutledge S, Dodd MB, Six J, Schipper LA (2015) Root carbon inputs under moderately diverse sward and conventional ryegrass-clover pasture: implications for soil carbon sequestration. Plant Soil. doi:10.1007/s11104-015-2463-z

Meng F, Dungait JAJ, Zhang X, He M, Guo Y, Wu W (2013) Investigation of photosynthate-C allocation 27 days after ^{13}C-pulse labeling of *Zea mays* L. at different growth stages. Plant Soil 373:755–764

Micwood AJ, Boutton TW (1998) Soil carbonate decomposition by acid had little effect on the $\delta^{13}C$ or organic matter. Soil Biol Biochem 30:1301–1307

Morrissey E, Gillespie J, Morina J, Franklin RB (2014) Salinity affects microbial activity and soil organic matter content in tidal wetland. Glob Chang Biol 20:1351–1362

Munns R, Tester M (2008) Mechanisms of salinity tolerance. Annu Rev Plant Biol 59:651–681

Nicolás C, Kennedy JN, Hernández T, García C, Six J (2014) Soil aggregation in a semiarid soil amended with composted and non-composted sewage sludge-Afield experiment. Geodema 219–220:24–31

Pausch J, Tian J, Riederer M, Kuzyakov Y (2013) Estimation of rhizodeposition at field scale: upscaling of a ^{14}C labeling study. Plant Soil 364:273–285

Qiu SJ, Ju XT, Ingwersen J, Qin ZC, Li L, Streck T, Christie P, Zhang FS (2010) Changes in soil carbon and nitrogen pools after shifting from conventional cereal to greenhouse vegetable production. Soil Tillage Res 107:80–87

Rangel-Castro JI, Prosser JI, Scrimgeour CM, Smith P, Ostle N, Ineson P, Meharg A, Killham K (2004) Carbon flow in an upland grassland: effect of liming on the flux of recently photosynthesized carbon to rhizosphere soil. Glob Chang Biol 10:2100–2108

Rennenberg H, Loreto F, Polle A, Brilli F, Fares S, Beniwal RS, Gessler A (2006) Physiological responses of forest trees to heat and drought. Plant Biol 8:556–571

Richert M, Saarnio S, Juutinen S, Silvola J, Augustin J, Merbach W (2000) Distribution of assimilated carbon in the system *Phragmites australis*-waterlogged peat soil after carbon-14 pulse labelling. Biol Fertil Soils 32:1–7

Saidy AR, Smernik RJ, Baldock JA, Kaiser K, Sanderman J, Macdonald LM (2012) Effects of clay mineralogy and

hydrous iron oxides on labile organic carbon stabilization. Geoderma 173–174:104–110

Salvo L, Hernández J, Ernst O (2010) Distribution of soil organic carbon in different size fractions, under pasture and crop rotations with conventional tillage and no-till systems. Soil Tillage Res 109:116–122

Schmitt A, Pausch J, Kuzyakov Y (2013) C and N allocation in soil under ryegrass and alfalfa estimated by ^{13}C and ^{15}N labeling. Plant Soil 368:581–590

Six J, Conant RT, Paul EA, Paustian K (2002) Stabilization mechanisms of soil organic matter: Implications for C-saturation of soils. Plant Soil 241:155–176

Toosi ER, Doane TA, Horwath WR (2012) Abiotic solubilization of soil organic matter, a less-seen aspect of dissolved organic matter production. Soil Biol Biochem 50:12–21

Torn MS, Kleber M, Zavaleta ES, Zhu B, Field CB, Trumbore SE (2013) A dual isotope approach to isolate soil carbon pools of different turnover times. Biogeosciences 10:8067–8081

Wang S, Xu J, Zhou C (2002) Using remote sensing to estimate the change of carbon storage: a case study in the estuary of Yellow River Delta. Int J Remote Sens 23:1565–1580

Wang W, Liu J, Zhang B, Zhang J, Li X, Y Y (2015) Critical evaluation of particle size distribution models using soil data obtained with a laser diffraction method. Soil Sci 178: 194–204

Wang ZY, Xin YZ, Gao DM, Li FM, Morgan J, Xing BS (2010) Microbial community characteristics in a degraded wetland of the Yellow River Delta. Pedosphere 20: 466–478

Warembourg FR, Estelrich HD (2001) Plant phenology and soil fertility effects on below-ground carbon allocation for an annual (*Bromus madritensis*) and a perennial (*Bromus erectus*) grass species. Soil Biol Biochem 33:1291–1303

Wong VNL, Greene RSB, Dalal RC, Murphy BW (2010) Soil carbon dynamics in saline and sodic soils: a review. Soil Use Manag 26:2–11

Xiao C, Janssens I A,, Liu P, Zhou Z, Sun OJ (2007) Irrigation and enhanced soil carbon input effects on below-ground carbon cycling in semiarid temperate grasslands. New Phytol 174: 835–846

Yadav S, Irfan M, Ahmad A, Hayat S (2011) Causes of salinity and plant manifestations to salt stress: A review. J Environ Biol 32:667–685

Zeller B, Dambrine E (2011) Coarse particulate organic matter is the primary source of mineral N in the topsoil of three beech forests. Soil Biol Biochem 43:542–550